



Research Paper

Therapeutic effect of Sirtuin 3 on ameliorating nonalcoholic fatty liver disease: The role of the ERK-CREB pathway and Bnip3-mediated mitophagy

Ruibing Li^{a,1}, Ting Xin^{b,1}, Dandan Li^a, Chengbin Wang^{a,*}, Hang Zhu^{a,*}, Hao Zhou^{a,c,**}

^a Chinese PLA General Hospital, Medical School of Chinese PLA, Beijing, PR China

^b Department of Cardiology, Tianjin First Central Hospital, Tianjin 300192, PR China

^c Center for Cardiovascular Research and Alternative Medicine, Wyoming University, Laramie, WY 82071, USA

ARTICLE INFO

Keywords:

Nonalcoholic fatty liver disease
Mitophagy
Bnip3
Sirt3
ERK-CREB signalling pathway

ABSTRACT

Increased mitochondrial damage is related to the progression of a diet-induced nonalcoholic fatty liver disease. The aim of our study is to investigate the role of Sirtuin 3 (Sirt3) in treating nonalcoholic fatty liver disease with a focus on mitophagy and the ERK-CREB pathway. Our data indicated that Sirt3 was downregulated in liver tissue in response to chronic HFD treatment. Interestingly, re-introduction of Sirt3 protected hepatic function, attenuated liver fibrosis, alleviated the inflammatory response, and prevented hepatocyte apoptosis. Molecular investigations demonstrated that lipotoxicity was associated with an increase in mitochondrial apoptosis as evidenced by reduced mitochondrial potential, augmented ROS production, increased cyt-c leakage into the nucleus, and activated caspase-9 apoptotic signalling. Additionally, Sirt3 overexpression protected hepatocytes against mitochondrial apoptosis via promoting Bnip3-required mitophagy. Functional studies showed that Sirt3 reversed Bnip3 expression and mitophagy activity via the ERK-CREB signalling pathway. Blockade of the ERK-CREB axis repressed the promotive effects of Sirt3 on Bnip3 activation and mitophagy augmentation, finally negating the anti-apoptotic influences of Sirt3 on hepatocytes in the setting of high-fat-stress. Collectively, our data show that high-fat-mediated liver damage is associated with Sirt3 downregulation, which is followed by ERK-CREB pathway inactivation and Bnip3-mediated inhibition of mitophagy, causing hepatocytes to undergo mitochondria-dependent cell death. Based on this, strategies for enhancing Sirt3 activity and activating the ERK-CREB-Bnip3-mitophagy pathways could be used to treat nonalcoholic fatty liver disease.

1. Introduction

Nonalcoholic fatty liver disease (NAFLD) encompasses a broad spectrum, including simple steatosis, nonalcoholic steatohepatitis (NASH) with fibrosis, cirrhosis, and probably hepatocellular carcinoma [1,2]. Approximately 30% of the U.S population is obese, and 75% of these obese individuals have NAFLD [3,4]. Pathogenically, increased free fatty acid levels have been associated with the development and progression of NAFLD [5]. Excessive free fatty acids enhance the oxidation of fatty acids in the liver, producing excessive superoxide [6]. Subsequently, uncontrolled oxidative stress disrupts mitochondrial function, causes membrane structure oxidation and generates most advanced oxidation protein products [7,8]. Among those pathological processes, mitochondrial dysfunction has been acknowledged as the primary molecular event of high-fat-mediated hepatocyte injury [9,10].

Damaged mitochondria fail to produce enough ATP to ensure normal hepatocyte function, resulting in disorders in lipid metabolism regulation, blood glucose management, and protein synthesis and output [11]. Moreover, damaged mitochondria contribute to oxidative stress, causing hepatocyte senescence [12,13]. More severely, poorly structured mitochondria could liberate pro-apoptotic factors into the cytoplasm/nucleus, initiating mitochondria-dependent hepatocyte death [14,15]. Accordingly, understanding the molecular mechanisms by which hyperlipidaemia imposes damage on mitochondria is significant for designing a novel approach to treat fatty liver disease.

Sirtuin 3 (Sirt3), a type of NAD-dependent deacetylase expressed mainly in mitochondria, has recently been reported to have multiple effects on mitochondrial protection in response to several types of stress, such as oxidative stress, hyperglycaemia, fatty acid composition, and myocardial infarction [16–18]. In fatty liver disease, Sirt3

* Corresponding authors.

** Corresponding author at: Chinese PLA General Hospital, Medical School of Chinese PLA, Beijing, PR China.

E-mail addresses: wangchengbin301@126.com (C. Wang), zcb1225@163.com (H. Zhu), zhouhao301@outlook.com, hzhou3@uwyo.edu (H. Zhou).

¹ These authors contributed equally to this study.

activation has been reported to promote acylcarnitine metabolism [19]. Moreover, in hepatitis B virus infection, Sirt3 could restrict HBV transcription and replication, limiting inflammation-mediated liver damage [20,21]. In liver ischaemia-reperfusion injury, Sirt3 is unfortunately downregulated, whereas exogenous administration of Sirt3 attenuates reperfusion-mediated liver damage via maintaining mitochondrial calcium homeostasis and energetic balance [22,23]. Along with the well-documented beneficial role of Sirt3 in liver protection, the relationship between Sirt3 and high-fat-mediated mitochondrial damage in fatty liver disease should be investigated.

Although mitochondria are susceptible to hyperlipidaemia-triggered damage, mitochondria can employ lysosomes to remove damaged mitochondrial fragments, which is termed mitophagy, a kind of mitochondrial autophagy [24,25]. This concept has been verified by our previous studies showing that mitophagy activation sustains mitochondrial energy metabolism [26], attenuates high lipid-mediated oxidative stress [27], prevents hyperlipidaemia-mediated mitochondrial apoptosis [28] and, as a result, inhibits the progression of fatty liver disease [29]. Furthermore, mitophagic activity is primarily regulated by Bnip3 [30], and deletion of Bnip3 has been found to be related to chronic liver damage and metabolic disorder. For example, in diabetic mice, Bnip3 deficiency aggravates insulin resistance and metabolic syndrome [31]. Moreover, Bnip3 deletion increases ROS production, the inflammatory response and steatohepatitis in the liver tissue [32]. Along with the well-documented role of Bnip3-mediated mitophagy in liver protection, we ask whether Bnip3-mediated mitophagy is regulated by Sirt3 in the setting of fatty liver disease.

Additionally, several pieces of evidence have established the upstream mediators of mitophagy activation, including the ERK-CREB signalling pathway. In chronic cardiovascular disorders, activation of the ERK-CREB signalling pathway sustains mitophagy activity [33], repressing cardiac fibrosis. Furthermore, in neuroinflammation, increased ERK is associated with high Bnip3 expression and mitophagy activation, protecting neurons against inflammation-mediated apoptosis [34]. However, no study is available to explain the role of the ERK-CREB signalling pathway in fatty liver disease and mitophagy management. Accordingly, the aim of our study is to explore the therapeutic effect of Sirt3 in fatty liver disease, especially focusing on hepatocyte mitochondrial apoptosis, Bnip3-mediated mitophagy, and the ERK-CREB signalling pathway.

2. Materials and methods

2.1. Animals and treatment

All animal protocols were approved by the Institutional Animal Care and Use Committee of the Institute of Model Animals of Chinese PLA General Hospital and the Animal Care and Use Committee of Chinese PLA General Hospital. Sirt3 transgenic (Sirt3-TG) mice (C57BL/6 background) purchased from Jackson Laboratory (Bar Harbor, ME, USA) were used to establish the fatty liver disease model. WT mice were used as the control group. Mice were housed in a temperature-controlled environment ($23 \pm 2^\circ\text{C}$) with a 12 h light/dark cycle. Male mice of 8–10 weeks were incorporated into the experiments and were continuously fed either a high-fat diet (HFD) or a normal chow (low-fat diet (LFD)) diet for 12 weeks according to our previous study [29].

2.2. Mouse serum cytokine and hepatic lipid analyses

For analysis of serum cytokine levels, the serum concentrations of cytokines were determined using ELISA. ELISA Kits (#PMTA00B for insulin, #PMLB00C for glucagon, #PMLB00C for C-Peptide, #PM4000B for TNF α , #PM6000B for MCP-1; Cusabio Technology, Wuhan, China) and commercial kits for triglyceride (TG) and total cholesterol (TC) (290-63701 for TG, 294-65801 for TC; Wako, Tokyo, Japan) were used to measure the TG and TC contents, according to the

manufacturer's instructions [35]. Liver functions were evaluated in the animals by determining the serum concentrations of alanine aminotransferase (ALT) and aspartate aminotransferase (AST) using an ADVIA 2400 Chemistry System analyser, according to the manufacturer's instructions [36].

2.3. Histological analysis

Liver sections were embedded in paraffin and then stained using haematoxylin and eosin (H&E) to visualise the hepatocyte swelling [37]. The hepatocyte vacuolation was evaluated via measuring the average diameter of hepatocyte. Lipid droplet accumulation in the liver was visualised using Oil Red O staining of frozen liver sections that were prepared in Tissue-Tek OCT compound. Relative Oil Red O accumulation was analysed by spectrophotometry (absorbance at 540 nm) according to a previous study [29]. For determination of liver fibrosis, Sirius Red staining was performed using paraffin-prepared liver sections. The average grayscale intensity was recorded using Image-Pro Plus 6.0 software [38]. The histological features of the tissues were observed and imaged using a light microscope (Olympus, Tokyo, Japan) [39].

2.4. Cell isolation and culture

Primary hepatocytes from 6 to 8 week-old mice (WT mice and Sirt3-TG mice) were isolated via liver perfusion. Briefly, mice were anaesthetised with pentobarbital sodium (90 mg/kg). A total of 45 ml of Liver Perfusion Medium (Life Technologies, Carlsbad, CA, USA, 17701-038) was perfused through the portal vein, followed by perfusion with Liver Digest Medium (Life Technologies, 17703-034) for 5 min at a rate of 2 ml/min. After this digestion, the liver was excised, minced and filtered through a steel mesh. Primary hepatocytes were separated via centrifugation at 50 g for 5 min and purified in 50% Percoll solution (17-0891-01, GE Healthcare Life Sciences, Buckinghamshire, England). Hepatocytes were cultured in Dulbecco's modified Eagle's medium supplemented with 10% foetal bovine serum and 1% penicillin-streptomycin in a 5% CO₂/water-saturated incubator at 37 °C. Palmitic acid (PA, 75 $\mu\text{mol/L}$; Sigma-Aldrich) was added to the medium for 24 h to establish an in vitro model of lipid accumulation in hepatocytes [29].

2.5. Western blotting analysis

Proteins were separated using 10% SDS-PAGE gels (#NP0301BOX, Invitrogen) and then transferred to PVDF membranes (#IPVH00010, Millipore). After the membranes were blocked in 5% skim milk, they were incubated overnight at 4 °C with primary antibodies and then for 1 h at room temperature with the corresponding secondary antibodies. A ChemiDoc MP Imaging System was used for signal detection [40]. Protein expression levels were quantified using Image Lab software and normalised to the levels of β -actin, which was used as a loading control. The primary antibodies used for immunoblotting were as follows: pro-caspase-3 (1:1000, Cell Signalling Technology, #9662), cleaved caspase-3 (1:1000, Cell Signalling Technology, #9664), Bax Monoclonal Antibody (6A7) (1:1000, Thermo Fisher Scientific, #14-6997-81), Bcl2 (1:1000, Cell Signalling Technology, #3498), caspase-9 (1:1000, Abcam #ab32539), LC3II (1:1000, Cell Signalling Technology, #3868), LC3I (1:1000, Cell Signalling Technology, #4599), Atg5 (1:1000, Cell Signalling Technology, #12994), p-ERK (1:1000, Abcam, #ab176660), t-ERK (1:1000, Abcam #ab54230), cyt-c (1:1000; Abcam; #ab90529), c-IAP (1:1000, Cell Signalling Technology, #4952), t-CREB (1:1000, Cell Signalling Technology, #9197), p-CREB (1:1000, Cell Signalling Technology, #9198), complex III subunit core (CIII-core2, 1:1000, Invitrogen, #459220), complex II (CII-30, 1:1000, Abcam, #ab110410), complex IV subunit II (CIV-II, 1:1000, Abcam, #ab110268), complex I subunit NDUFB8 (CI-20, 1:1000, Abcam, #ab110242), TNF α (1:1000, Abcam, #ab6671), TGF β (1:1000, Abcam, #ab92486), MCP1 (1:1000,

Abcam, #ab25124), IL6 (1:1000, Abcam, #ab7737), MMP9 (1:1000, Abcam, #ab38898), Bnip3 (1:1000, Cell Signalling Technology, #44060) Sirt3 (1:1000, Abcam, no. ab86671), Tom20 (mitochondria marker, 1:1000, Abcam, #ab186735).

2.6. Immunofluorescent staining and mitophagy detection

Cells were first fixed with 4% paraformaldehyde for 30 min at room temperature. After incubation with 3% hydrogen peroxide for 10 min to block endogenous peroxidase activity, the samples were treated with the primary antibodies at 4 °C overnight. After the slides were washed with PBS and then incubated with secondary antibody (1:500, Invitrogen, Carlsbad, CA, USA) at room temperature for 45 min. Nuclei were stained using DAPI. Images were observed with fluorescence microscopy (Olympus BX-61). The primary antibodies used in the present study were as follows: p-ERK (1:1000, Abcam, #ab176660), Bnip3 (1:1000, Cell Signalling Technology, #44060), Tom20 (mitochondria marker, 1:1000, Abcam, #ab186735), LAMP1 (lysosome marker, 1:1000, Abcam, #ab24170), cyt-c (1:1000; Abcam; #ab90529). Mitophagy is the result of fusion between mitochondria and lysosome. The green mitochondria locate with red lysosome would generate the orange mitophagy. Then, the number of orange dot was measured to quantify the number of mitophagy.

2.7. Adenovirus vector construction and small interfering RNA (siRNA) knockdown

For Sirt3 overexpression, the entire coding region of the mouse Sirt3 gene was placed into a replication-defective adenoviral vector under the control of the cytomegalovirus promoter. Recombinant adenoviruses were generated using an AdEasy vector kit (Stratagene, La Jolla, California, USA). Plasmids were recombined with the pAdEasy backbone vector according to the manufacturer's instructions [41] and were used to transfect HEK293T cells with the aid of FuGENE transfection reagent (E2312, Roche, Indianapolis, IN, USA). Recombinant adenoviruses were plaque-purified, titred to 10⁹ plaque-forming units per ml and verified via restriction digestion. The cells were infected with adenoviruses in diluted medium at a multiplicity of infection of 50 for 24 h.

Knockdown experiments of Bnip3 in mouse primary hepatocytes were performed using siRNA oligonucleotides from GenePharma, China. The cells were transfected with siRNAs using Lipofectamine RNAiMAX (cat. 13778030, Life Technologies) [42].

2.8. ROS staining

ROS production was quantified ex vivo by DCFDA staining. Isolated cells were incubated with 5 mg/ml DCFDA in complete DMEM medium for 30 min, washed with phosphate-buffered saline, and analysed by flow cytometry [43]. For each experiment, at least 1 × 10⁵ cells were analysed to calculate the mean fluorescence intensity of DCFDA staining.

2.9. GSH, GPx and SOD detection

GSH, GPx and SOD are important antioxidants that scavenge free radicals and, therefore, suppress the extent of oxidative stress. The SOD/GPx activity and GSH concentration were measured using commercial kits (Beyotime Institute of Biotechnology, China) following the manufacturer's instructions [44].

2.10. Cellular viability detection and apoptosis assays

Cellular viability detection and apoptosis assays were measured via MTT assays and TUNEL staining [45]. The MTT assay was conducted as previously described. Briefly, the cells were seeded in a 96-well plate at

37 °C with 5% CO₂. Subsequently, 20 μl 3-(4,5-dimethylthiazol-2-yl)-2,5-diphenyltetrazolium bromide (MTT) (5 mg/ml; pH 7.4; Sigma-Aldrich) was added to the cells for 4 h. The supernatants were then discarded, and 100 μl dimethyl sulfoxide (Sigma-Aldrich) was added to each well for 10 min. The OD of the samples was measured at an absorbance of 490 nm using a spectrophotometer (Epoch 2; BioTek Instruments, Inc., Winooski, VT, USA). The assay was repeated 3 times.

A TUNEL assay was performed using a one-step TUNEL kit (Beyotime Institute of Biotechnology, Haimen, China) according to the manufacturer's instructions. TUNEL staining was performed with fluorescein-dUTP (Invitrogen; Thermo Fisher Scientific, Inc.) to stain apoptotic cell nuclei, and DAPI (5 mg/ml) was used to stain all cell nuclei at room temperature for 3 min. The cells in which the nucleus was stained with fluorescein-dUTP were defined as TUNEL positive. The slides were then imaged under a confocal microscope.

2.11. Mitochondrial function measurement

Mitochondrial function measurement was performed by analysing ATP production and mitochondrial potential [46]. The cellular ATP levels were measured using a firefly luciferase-based ATP assay kit (Beyotime Institute of Biotechnology). The mitochondrial transmembrane potential was analysed using a TMRE Kit (Invitrogen; Thermo Fisher Scientific, Inc., cat. no. T669). Results were analysed using a spectrophotometer (Epoch 2; BioTek Instruments, Inc., Winooski, VT, USA) [47].

2.12. Statistical analysis

All statistical analyses were performed using SPSS software (version 19.0). All data in this study are expressed as the mean ± SEM. Several experiments were performed blind such as mouse serum cytokine detection, hepatic lipid analyses, histological analysis, mitochondrial function measurement, cellular viability detection, immunofluorescence, and ROS staining. For data that showed a normal distribution and homogeneity of variance, one-way ANOVA was performed for comparisons among more than two groups using a Bonferroni analysis. P value < 0.05 was considered significant.

3. Results

3.1. Sirt3 overexpression prevents diet-mediated fatty liver disease

To verify the alterations of Sirt3 in the fatty liver disease, we fed mice a high-fat diet (HFD) for 12 weeks to generate fatty liver disease. The change of Sirt3 was monitored via western blotting. As shown in Fig. 1A–B, HFD significantly reduced the expression of Sirt3 in liver tissue compared to that the low-fat-diet (LFD) group. To test whether Sirt3 directly influenced the progression of fatty liver disease, we treated Sirt3 transgenic (Sirt3-TG) mice with the HFD. Subsequently, the hepatic lipid metabolism parameters were measured. Compared to the low-fat diet (LFD), the HFD increased the body weights (Fig. 1C) and liver weights (Fig. 1D); these effects were reversed by Sirt3 overexpression. In addition, compared to the LFD, the HFD increased the levels of fasting blood glucose (Fig. 1E), c-peptide (Fig. 1F), HbA1c (Fig. 1G), and glucagon (Fig. 1H). However, these alterations were attenuated in Sirt3-TG mice.

Regarding hepatic damage parameters, the levels of triglycerides (Fig. 1I), total cholesterol (Fig. 1J), leptin (Fig. 1K), adiponectin (Fig. 1L) alanine transaminase (ALT) (Fig. 1M), and aspartate transaminase (AST) (Fig. 1N) were upregulated in HFD-treated mice and were downregulated in Sirt3-TG mice. Altogether, this information indicates that Sirt3 is downregulated in response to HFD and that overexpression of Sirt3 prevents diet-mediated fatty liver disease.

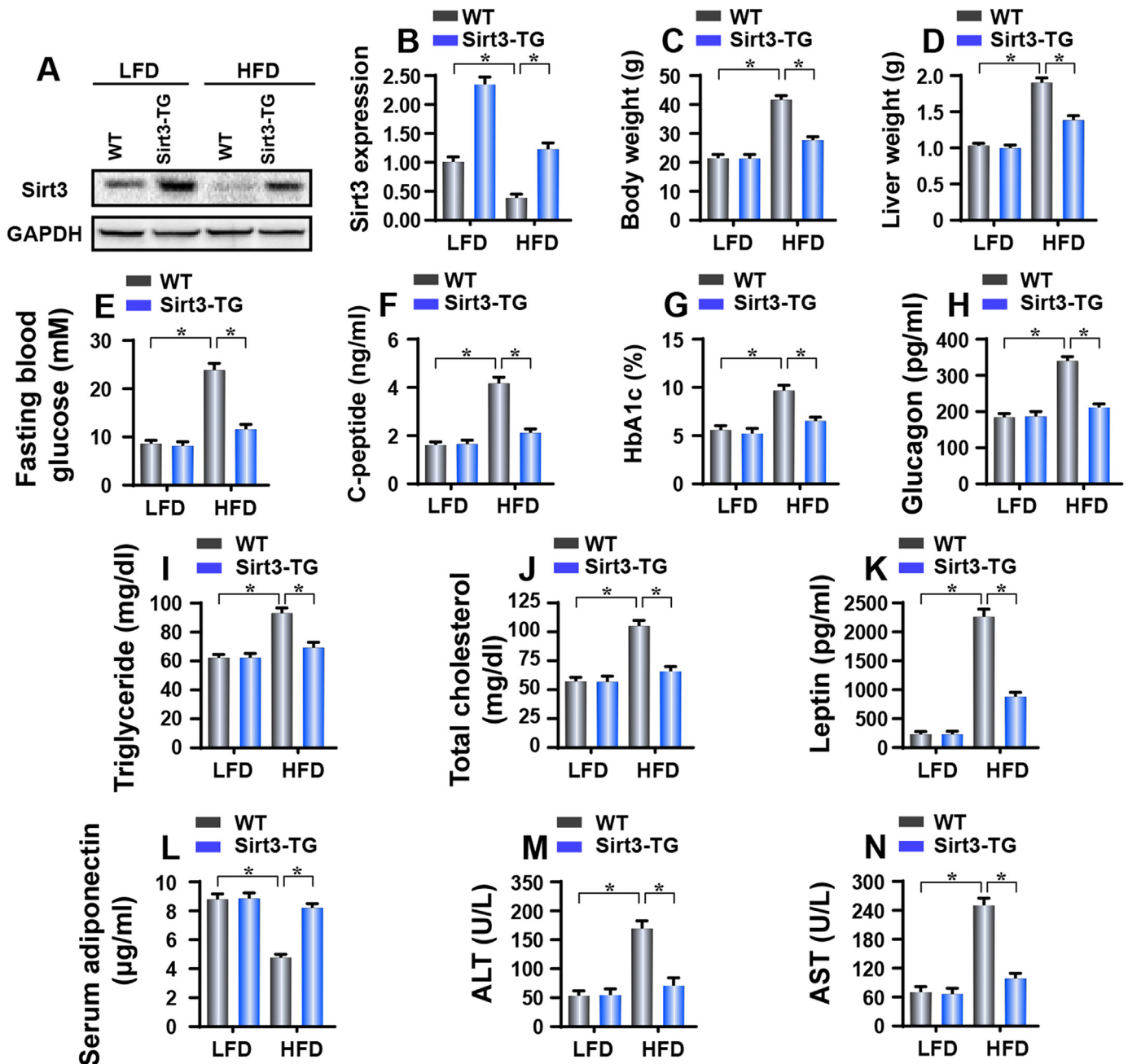


Fig. 1. Sirt3 represses HFD-induced fatty liver disease. A–B. Representative western blot of Sirt3 expression in the liver tissues from WT mice and Sirt3 transgenic (Sirt3-TG) mice. C. Body weights of WT mice and Sirt3-TG mice treated with LFD or HFD. D. Liver weights in WT mice and Sirt3-TG mice treated with LFD or HFD. E. The glucose levels in WT mice and Sirt3-TG mice in the presence of HFD. F–N. The levels of c-peptide, HbA1c, glucagon, triglyceride, total cholesterol, leptin, adiponectin, ALT and AST in the blood isolated from WT mice and Sirt3-TG mice using ELISA. The data represent the mean \pm SEM (n = 4 mice per group). *P < 0.05.

3.2. Sirt3 reduces hepatic damage induced by high-fat diet

Subsequent experiments were performed to analyse the liver histological alterations in response to Sirt3 overexpression in the presence of HFD treatment. As shown in Fig. 2A–B, HFD treatment increased the size of hepatocytes, as evaluated via H&E staining. However, this alteration was reversed by Sirt3 overexpression. Moreover, to observe the lipid accumulation in liver, we performed Oil Red O staining. The results in Fig. 2C–D demonstrated that HFD treatment promotes lipid accumulation in the liver, and this effect was reversed by Sirt3 overexpression. Additionally, liver fibrosis was measured via Sirius Red staining, and the results indicated that HFD-triggered liver fibrosis was

attenuated in Sirt3-TG mice (Fig. 2E–F). This finding was further verified via analysing fibrosis parameters using western blotting. As shown in Fig. 2G–J, Collagen I/III/IV were increased in response to HFD treatment and were reduced in Sirt3-TG mice. Furthermore, the pathways related to liver fibrosis, such as TGF β and MMP9 (Fig. 2K–L), were also upregulated in HFD-treated mice and were downregulated in Sirt3-TG mice. Altogether, these data suggest that Sirt3 acts as an endogenous defender against the HFD-mediated hepatocyte vacuolation, steatosis and fibrosis.

The liver inflammatory response was also evaluated because inflammation has been reported to be a primary cause of fatty liver disease. Through ELISA (Fig. 2M–O) and western blotting analysis

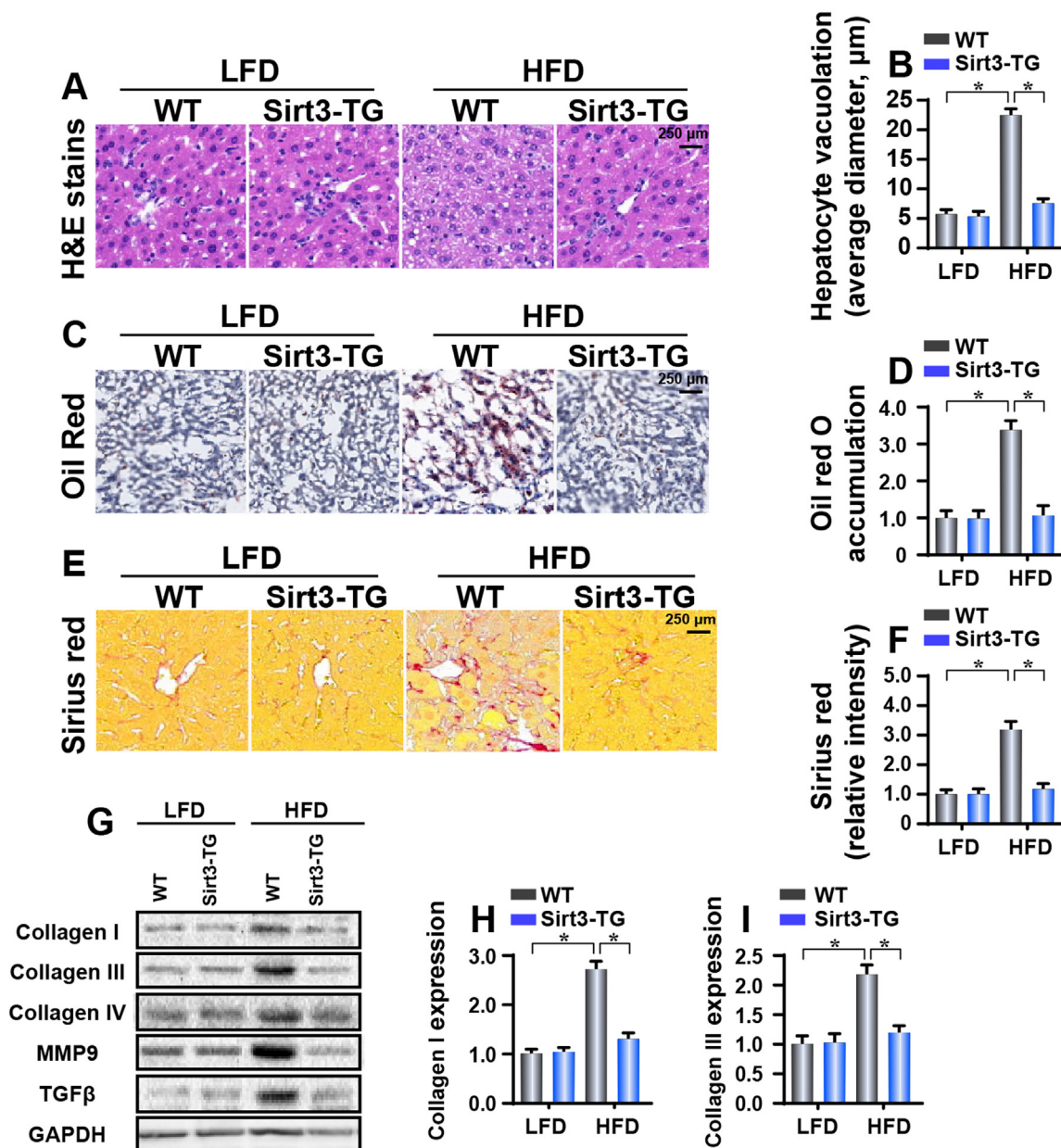


Fig. 2. Sirt3-TG mice are protected against HFD-induced chronic liver injury. A–B. Liver sections with haematoxylin and eosin (H&E) staining. C–D. Hepatosteatosis was revealed by Oil Red O staining. E–F. Hepatic fibrosis was revealed by Sirius Red staining. G–L. Western blotting was performed to analyse the expression of proteins related to liver fibrosis. M–O. The levels of inflammatory factors in the blood were evaluated via ELISA. P–S. The liver tissues of WT mice and Sirt3-TG mice were isolated and western blotting was carried out to analyse the expression of pro-inflammation factors. The data represent the mean \pm SEM (n = 4 mice per group). *P < 0.05.

(Fig. 2P–S), we demonstrated that inflammatory factors such as $\text{TNF}\alpha$, IL-8 and MCP1 were increased in HFD-fed mice and were reduced to near-normal levels in Sirt3-TG mice (Fig. 2M–S). Taken together, our data illustrate the inhibitory role played by Sirt3 in suppressing HFD-mediated hepatocyte damage.

3.3. Sirt3 attenuates hepatocyte death via sustaining mitochondrial function

Excessive lipid accumulation could induce hepatocyte death via disrupting mitochondrial function. Accordingly, the following experiments were performed to analyse the cellular viability in response to high-fat damage in vitro. Primary hepatocytes were isolated from WT and Sirt3-TG mice and were then treated with palmitic acid (PA, 75 $\mu\text{mol/L}$ for 24 h) in vitro. Subsequently, cellular viability was measured via MTT assays. As shown in Fig. 3A, PA treatment significantly

reduced hepatocyte viability, and this effect was reversed by Sirt3 overexpression. To understand the mechanism by which PA reduced cellular viability, we performed TUNEL assays to investigate the apoptotic index of hepatocytes in response to PA treatment. As shown in Fig. 3B–C, the number of TUNEL-positive cells was increased in the PA-loaded cells and was reduced to near-normal levels in the Sirt3-overexpressing cells. This information indicates that high-fat treatment promotes hepatocyte apoptosis, and this process is strongly blocked by Sirt3.

A previous study reported that mitochondrial damage is implicated in hyperlipidaemia-mediated hepatocyte apoptosis; thus, mitochondrial homeostasis was evaluated in the Sirt3-overexpressing cells in the presence of PA stress. First, mitochondrial ROS production was increased by PA treatment, as determined using flow cytometry analysis (Fig. 3D–E). However, Sirt3 overexpression repressed the ROS

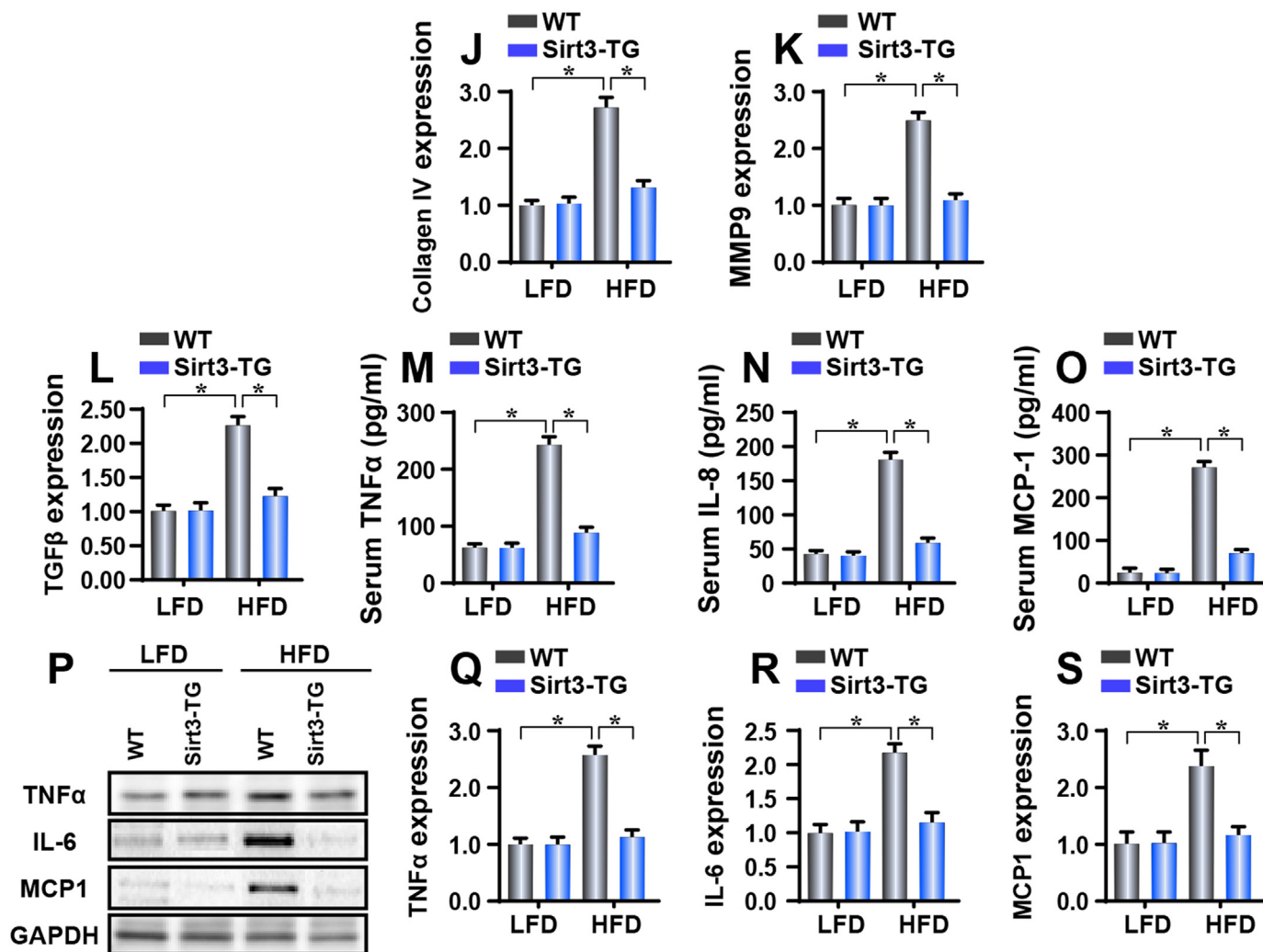


Fig. 2. (continued)

generation (Fig. 3D–E). As a consequence of ROS overproduction, the concentrations of antioxidants such as GSH, SOD and GPx were downregulated in PA-treated cells and were reversed to near-normal levels in the Sirt3-overexpressing cells (Fig. 3F–H).

Furthermore, based on previous findings, uncontrolled mitochondrial oxidative stress interrupts the ATP production in the mitochondria [48]. In the present study, we demonstrated that PA-suppressed ATP production was reversed by Sirt3 overexpression (Fig. 3I). Collectively, these results indicate that PA-evoked mitochondrial dysfunction is repressed by Sirt3 overexpression in hepatocytes.

3.4. Sirt3 blocks hepatocyte mitochondrial apoptosis in the setting of high-fat injury

At the molecular level, mitochondrial dysfunction is the early stage of cellular apoptosis [49]. Mitochondrial apoptosis is characterised by ATP shortage, mitochondrial potential collapse, pro-apoptotic factor liberation, and activation of the caspase family [50]. In the present study, the mitochondrial potential was reduced in response to PA treatment and was reversed to near-normal levels in the Sirt3-overexpressing cells (Fig. 4A). At the molecular levels, mitochondrial potential was stabilised via the mitochondrial respiratory complex. However, PA treatment reduced the expression of the mitochondrial respiratory complex, and this effect was reversed by Sirt3 overexpression (Fig. 4B–E). Mitochondrial potential reduction promotes pro-apoptotic factor leakage from the mitochondria into the cytoplasm/

nucleus [51]. To confirm this, we performed immunofluorescence assays. As shown in Fig. 4F–G, PA treatment promotes the cyt-c leakage into the cytoplasm/nucleus when compared to that of the control group. Cyt-c is the mitochondrial pro-apoptotic factor that activates caspase-9 and caspase-3 upon liberation from the mitochondria into the cytoplasm/nucleus. However, the PA-triggered cyt-c leakage was strongly inhibited by Sirt3 overexpression (Fig. 4F–G). As a consequence of cyt-c liberation, pro-apoptotic proteins such as caspase-3, caspase-9, and Bax were increased in PA-treated cell (Fig. 4H–M). By comparison, the contents of anti-apoptotic proteins such as Bcl-2 and survivin were correspondingly downregulated (Fig. 4H–M). Interestingly, re-introduction of Sirt3 corrected the balance between pro-apoptotic proteins and anti-apoptotic factors (Fig. 4H–M). Taken together, these data suggested that PA-initiated mitochondrial apoptosis was blocked by Sirt3 in hepatocytes.

3.5. Sirt3 activates mitophagy via upregulating Bnip3 expression

In response to mitochondrial damage, mitochondria themselves would activate mitophagy to remove the poorly structured mitochondria, maintaining mitochondrial quantity and quality [52]. To observe the mitophagy activity in response to PA, we performed western blotting. As shown in Fig. 5A–G, compared to the control group, PA treatment reduced the expression of LC3II and increased the expression of LC3I, indicative of the impairment of autophagosomes. Subsequently, mitochondria were isolated, and the mitochondrial LC3II

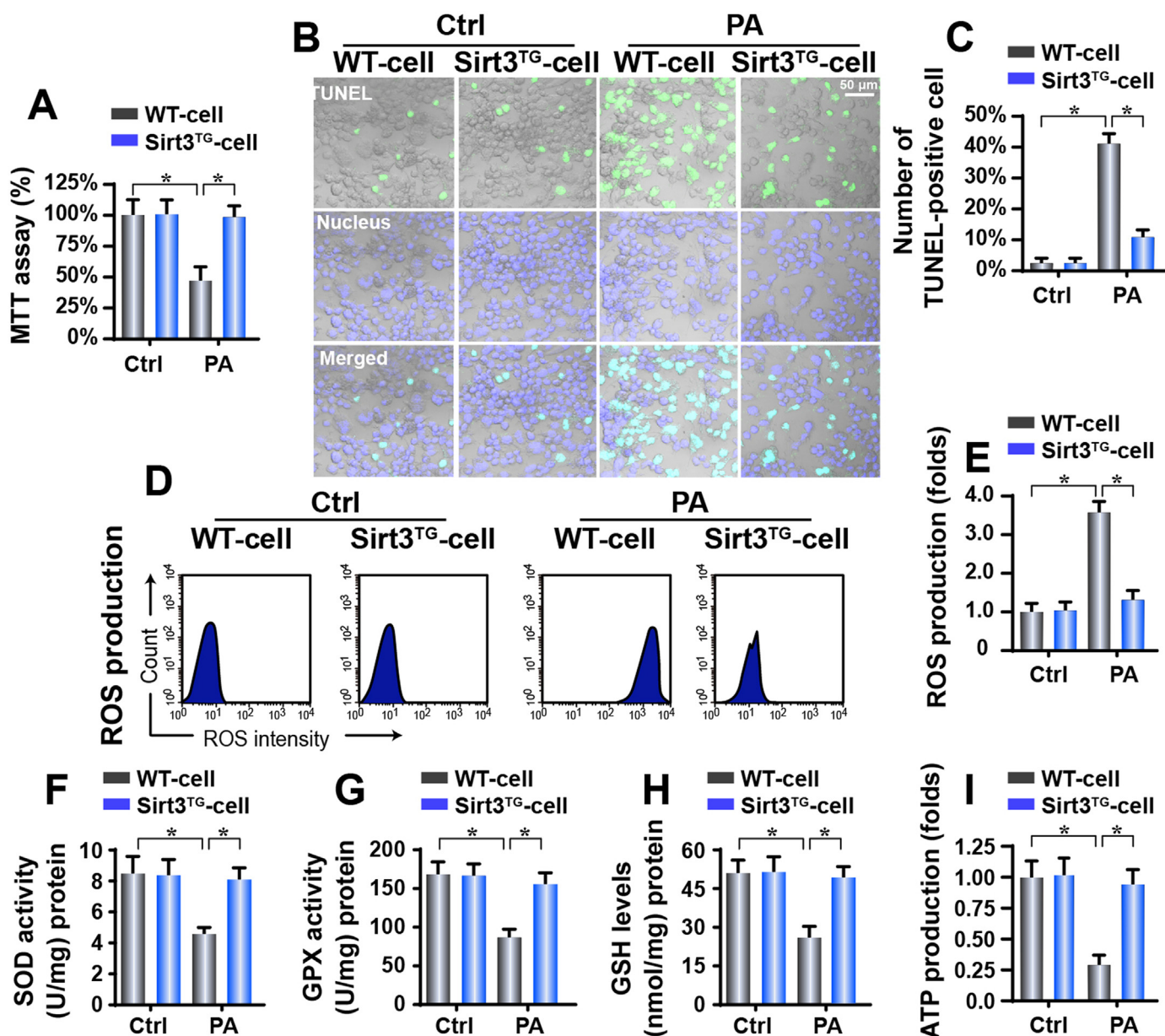


Fig. 3. Sirt3 alleviates high-fat-induced hepatocyte death. A. Primary hepatocytes were isolated from WT mice and Sirt3-TG mice. Then, PA was used in vitro to mimic the high-fat damage. MTT assay was used to analyse the hepatocyte viability in response to PA treatment. B–C. TUNEL staining for apoptosis detection. The green nucleus indicates an apoptotic cell. D–E. The ROS production in Sirt3-overexpressing cells with PA treatment was measured via flow cytometry. F–H. The levels of antioxidants, including SOD, GSH and GPx, were measured via ELISA. I. For analysis of mitochondrial function, cellular ATP production was evaluated via ELISA. The data represent the mean ± SEM (n = 4 mice per group). *P < 0.05.

(mito-LC3II) was measured. Similarly, the content of mito-LC3II was also repressed by PA when compared to that of the control group (Fig. 5A–G). Additionally, the mitophagy parameters, such as Beclin1 and Atg5, were also downregulated in response to PA treatment. Altogether, these data indicate that mitophagy is inactivated by PA in hepatocytes (Fig. 5A–G). Interestingly, regaining Sirt3 reversed the expression of mito-LC3II, Atg5 and Beclin1, suggestive of mitophagy activation in response to Sirt3 overexpression.

According to a previous study, mitophagy in hepatocytes is primarily regulated by Bnip3 [29]. In the present study, we found that Bnip3 expression was downregulated by PA treatment and was upregulated in the Sirt3-overexpressing cells (Fig. 5 A and G). This information suggests that Sirt3 reverses mitophagy activity that may occur via regulating Bnip3 expression. To further confirm whether Bnip3 is required for Sirt3-mediated mitophagy activation in the

presence of PA, we transfected siRNA against Bnip3 into the Sirt3-overexpressing cells. Subsequently, mitophagy activity was further observed via immunofluorescence. As shown in Fig. 5H–J, numerous mitochondria were co-located with lysosomes in the control group; however, PA treatment disrupted the fusion between mitochondria and lysosomes. Interestingly, overexpression of Sirt3 re-activated the interaction between mitochondria and lysosomes, and this effect was abrogated by deleting Bnip3 (Fig. 5H–J), indicating that Sirt3 maintained mitophagy via Bnip3. Altogether, our data indicate that mitophagy is drastically inhibited by PA and is re-activated by Sirt3 via reversing Bnip3 expression.

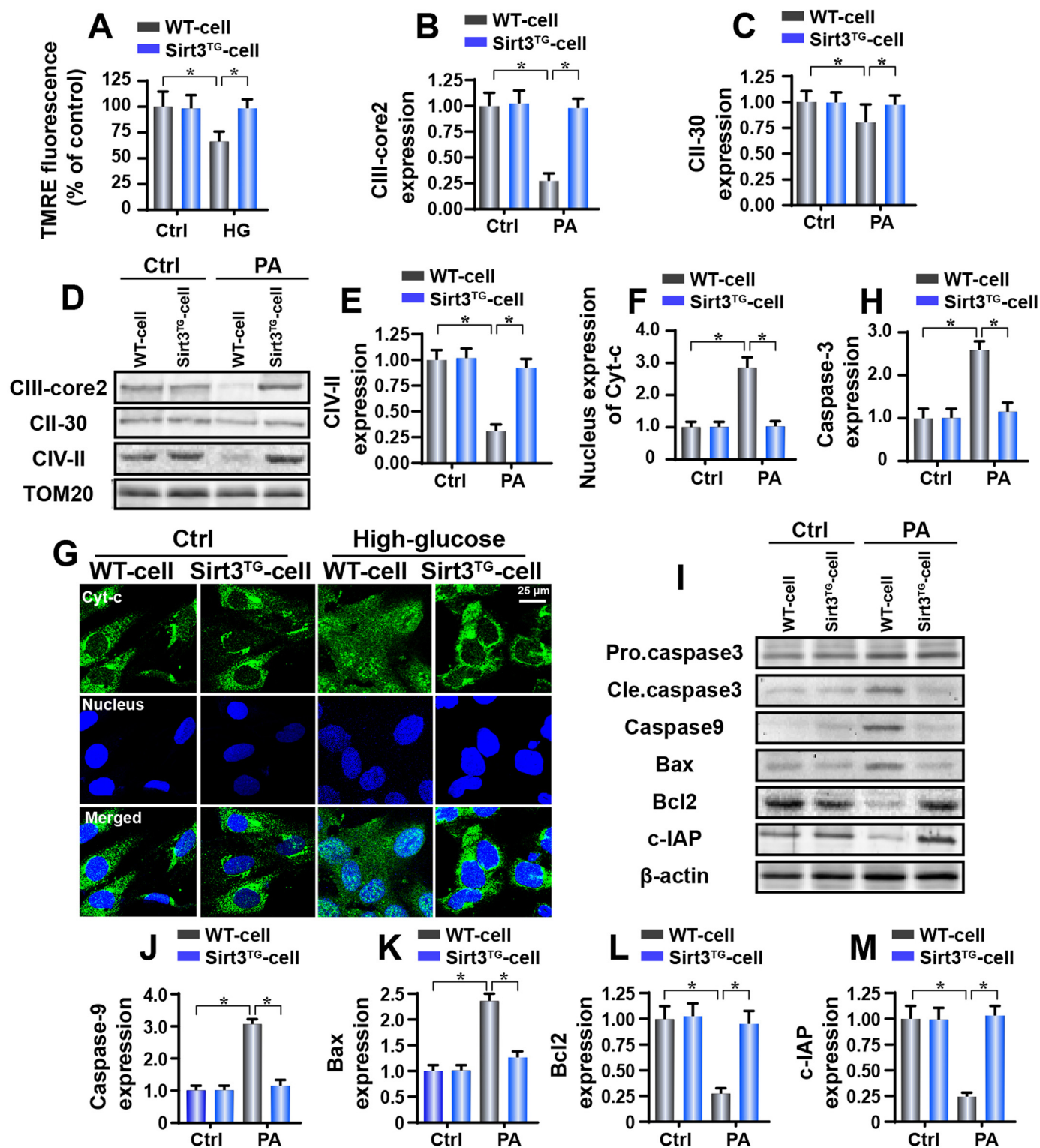


Fig. 4. Sirt3 sustains mitochondrial function and blocks mitochondrial apoptosis activation. **A.** The mitochondrial membrane potential was evaluated using TMRE. The relative TMRE fluorescence was evaluated using spectrophotometer. **B–E.** After PA treatment, hepatocytes were collected, and the proteins were isolated. Then, western blotting was performed to analyse the expression of the mitochondrial respiratory complex. Tom20 was the loading control for the mitochondrial proteins. **F–G.** Immunofluorescence assay for cyt-c liberation. DAPI was used to tag the nucleus. The fusion of cyt-c and DAPI indicates the leakage of cyt-c from mitochondria into the cytoplasm/nucleus. **H–M.** The anti-apoptotic and pro-apoptotic protein expression was detected to quantify the mitochondrial apoptosis using western blotting analysis. The data represent the mean ± SEM (n = 4 mice per group). *P < 0.05.

3.6. Bnip3-mediated mitophagy protects mitochondria against high-fat-mediated damage

To explain the beneficial effects of Bnip3-mediated mitophagy in

mitochondrial protection exerted by Sirt3, we examined the mitochondrial function again in Bnip3-knockout cells. First, the mitochondrial potential was reduced in the PA-treated cells and was stabilised in the Sirt3-overexpressing hepatocytes (Fig. 6A). However, loss

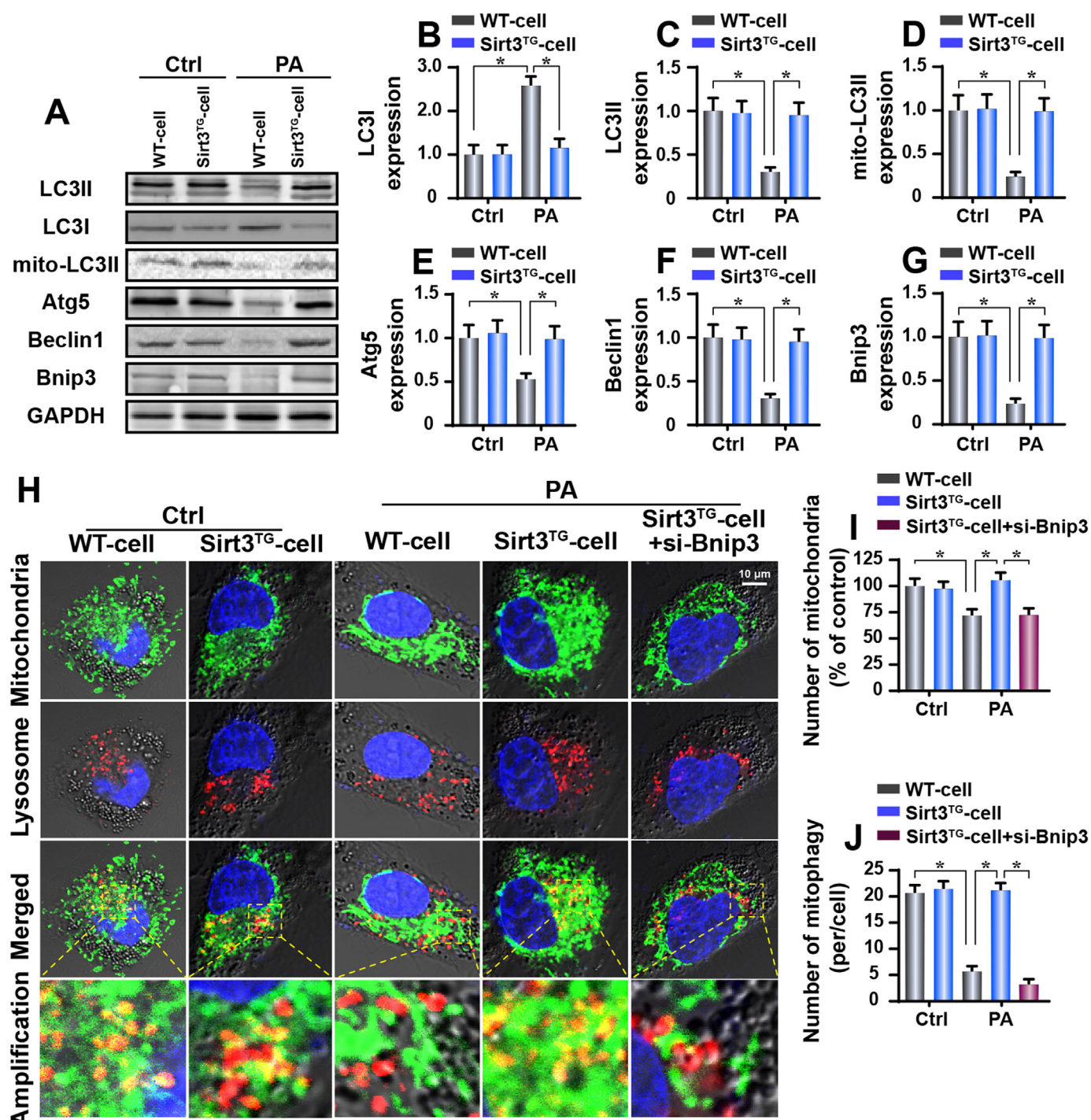


Fig. 5. Hyperlipemia-inhibited mitophagy is re-activated by Sirt3 overexpression via Bnip3. A–G. After PA treatment, hepatocytes were collected, and the proteins were isolated. Then, western blotting was performed to analyse the proteins expression related to mitophagy. H–J. Immunofluorescence assay for mitophagy. The location of mitochondria and lysosomes indicates mitophagy. The number of mitophagy events was recorded. The data represent the mean ± SEM (n = 4 mice per group). *P < 0.05.

of Bnip3 negated the protective effect of Sirt3 on mitochondrial potential stabilisation (Fig. 6A). In addition, Sirt3-inhibited cyt-c liberation was also reversed by Bnip3 deletion in hepatocytes treated with PA (Fig. 6B–C). Moreover, the concentration of antioxidants was increased by Sirt3 overexpression and was reduced in response to Bnip3 deletion (Fig. 6D–F). These data indicated that Sirt3 overexpression maintains mitochondrial function.

To verify whether Bnip3-mediated mitophagy suppresses PA-mediated hepatocyte mitochondrial apoptosis, we performed caspase-9

activity and LDH release assays. Caspase-9, the key marker of mitochondrial apoptosis, was activated by PA treatment and was inactivated by Sirt3 overexpression (Fig. 6G). However, the loss of Bnip3 increased the caspase-9 activity despite the overexpression of Sirt3 (Fig. 6G). Moreover, the content of LDH was increased in PA-loaded hepatocytes, indicative of the breakage of cell membranes due to cell death (Fig. 6H). However, Sirt3 overexpression reduced the LDH release, and this effect was dependent on Bnip3 expression. Besides, to observe the role of Bnip3-related mitophagy in lipid accumulation, we

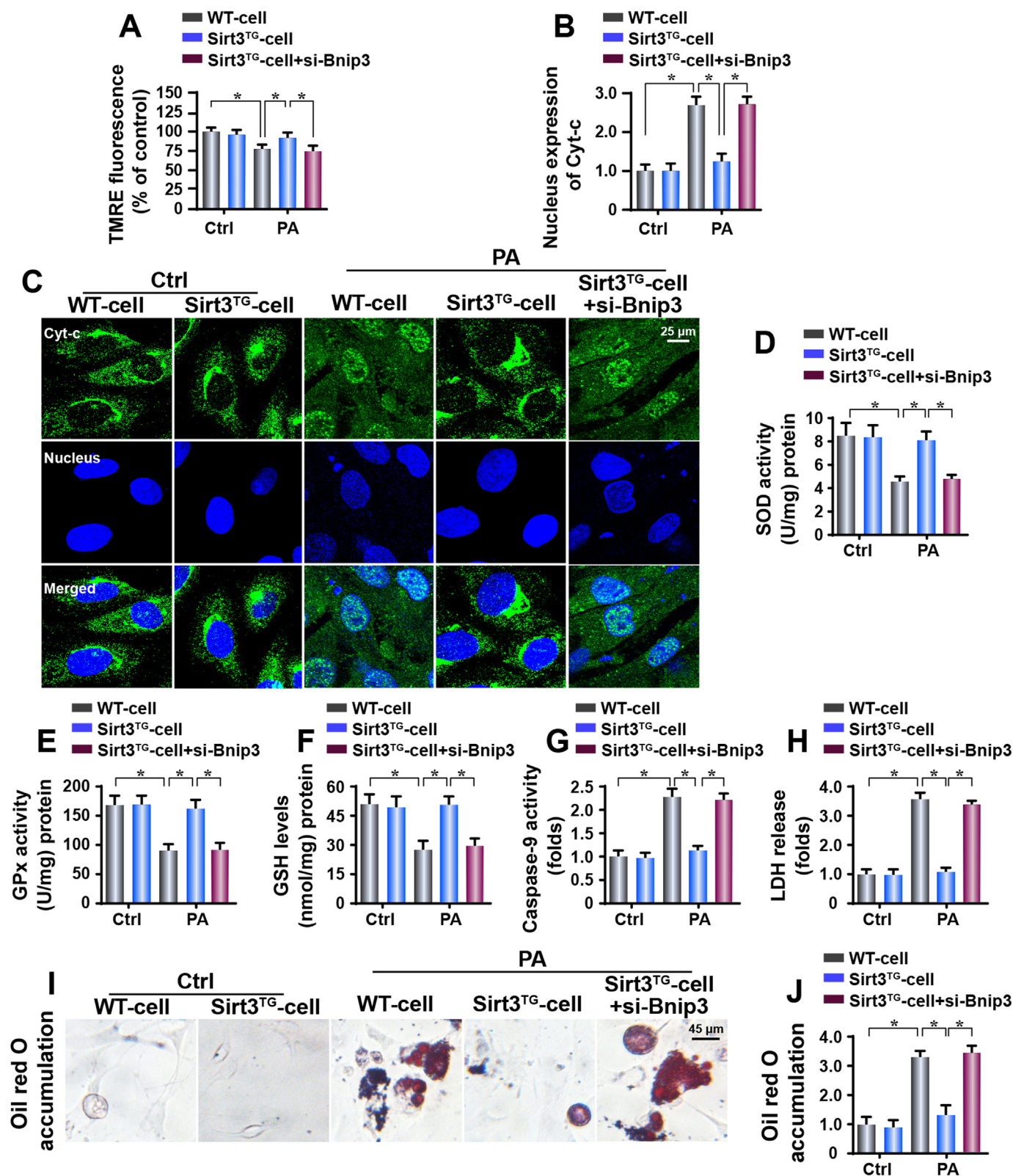


Fig. 6. Bnip3-mediated mitophagy preserves mitochondrial homeostasis. **A** The mitochondrial membrane potential was evaluated using TMRE. The relative TMRE fluorescence was evaluated using spectrophotometer. **B–C.** Cyt-c leakage into cytoplasm/nucleus was verified via immunofluorescence assay. The nucleus expression of cyt-c was recorded. **D–F.** The concentrations of antioxidants were measured via ELISAs. **G.** Caspase-9 activity was measured to reflect the role of Bnip3 deletion in cell apoptosis. **H.** LDH release assay was performed in Sirt3-overexpressing or Bnip3-knockout cells. **I–J.** Lipid accumulation was revealed by Oil Red O staining. The data represent the mean ± SEM (n = 4 mice per group). *P < 0.05.

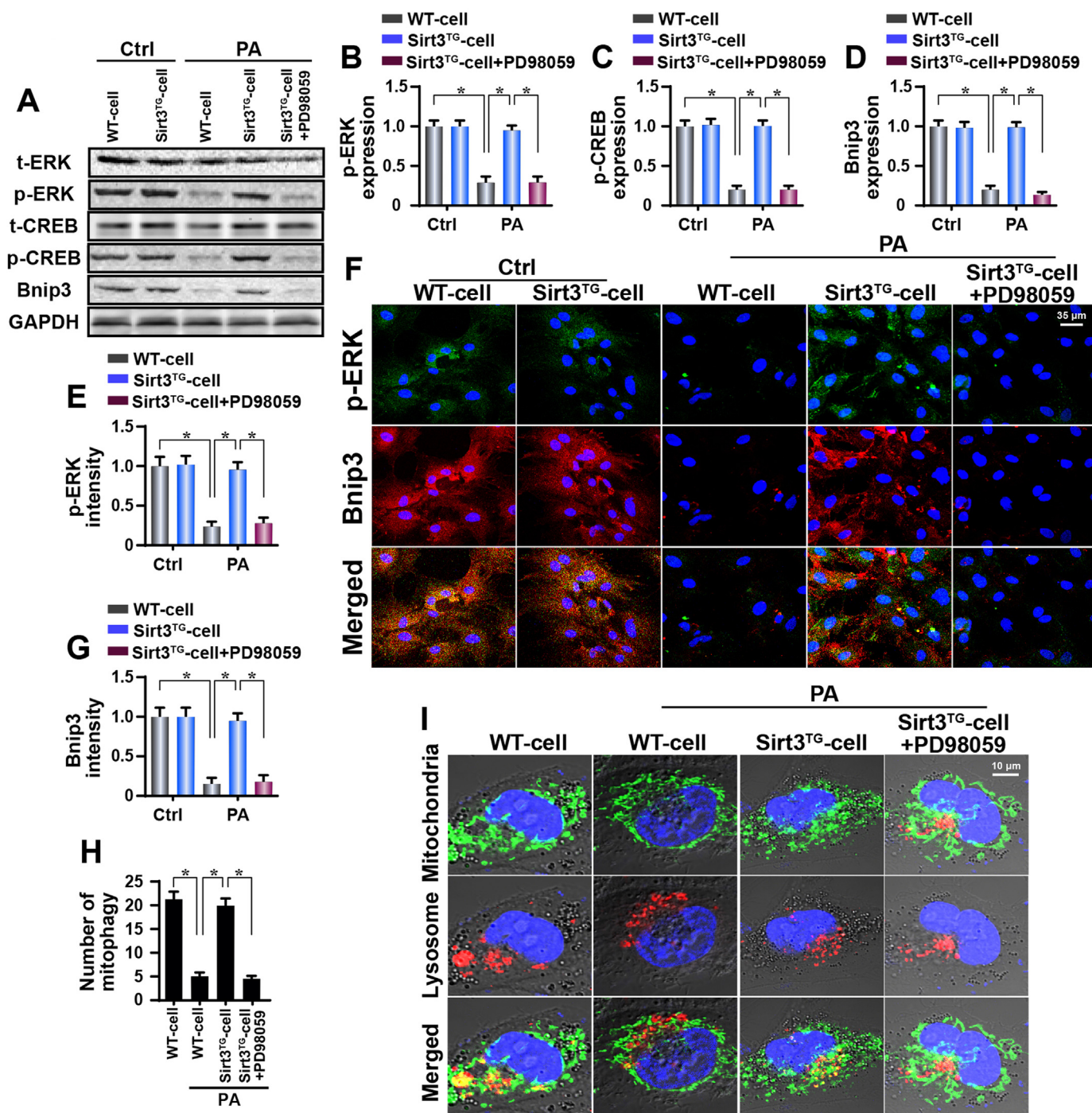


Fig. 7. Sirt3 modulates Bnip3 via the ERK-CREB signalling pathway. A–D. Proteins were isolated from PA-treated hepatocytes, and then, western blotting was carried out to analyse the expression of ERK phosphorylation, CREB phosphorylation and Bnip3. To inhibit the activity of ERK, PD98059 was applied to Sirt3-overexpressing cells. E–G. Immunofluorescence assay for ERK phosphorylation and Bnip3. PD98059 was used to block the ERK activation. H–I. The number of mitophagy events was monitored via immunofluorescence. The data represent the mean ± SEM (n = 4 mice per group). *P < 0.05.

performed Oil Red O staining in hepatocyte. The results in Fig. 6I–J demonstrated that Sirt3 overexpression inhibited PA-mediated lipid accumulation; this effect of which was negated by Bnip3 deletion.

3.7. Sirt3 controls Bnip3-mediated mitophagy via the ERK-CREB signalling pathway

To determine the mechanism by which Sirt3 modulates Bnip3 expression, we focused on the ERK-CREB signalling pathway since this cascade has been reported to be the upstream mediator of mitophagy in

cardiovascular disorders and neurological problems [33,34]. First, we demonstrated that the ERK-CREB pathway was inactivated by PA treatment, as evidenced by decreased phosphorylated ERK and CREB expression (Fig. 7A–D). Interestingly, Sirt3 overexpression reversed the levels of p-ERK content and p-CREB (Fig. 7A–D). To determine whether the ERK-CREB signalling pathway was involved in Sirt3-mediated Bnip3 upregulation, we used a pathway blocker. PD98059, an inhibitor of the ERK signalling pathway, not only inhibited Sirt3-mediated ERK and CREB activation but also repressed Sirt3-induced Bnip3 upregulation (Fig. 7A–D), indicating that the ERK-CREB pathway is responsible

for Sirt3-modulated Bnip3 elevation. This finding was further validated via immunofluorescence assays. The fluorescence intensities of p-ERK and Bnip3 were decreased in PA-treated hepatocytes and were reversed to near-normal levels in Sirt3-overexpressed cells (Fig. 7E–G). However, blockade of the ERK pathway significantly repressed Bnip3 expression despite the overexpression of Sirt3 (Fig. 7E–G). These data indicate that Sirt3 controls Bnip3 expression via the ERK-CREB signalling pathway.

Subsequently, to confirm whether the ERK-CREB axis was also involved in mitophagy activity, immunofluorescence for mitophagy was performed again. Compared to the control, PA repressed the cooperation between mitochondria and lysosomes, and this effect was reversed by Sirt3 overexpression (Fig. 7H–I). However, inhibition of the ERK-CREB signaling pathway abrogated the promotive effect of Sirt3 on mitophagy activation (Fig. 7H–I). Altogether, our data support the functional importance of the ERK-CREB signalling pathway in promoting Sirt3-modulated mitophagy in the setting of high-fat stress.

3.8. The ERK-CREB signalling pathway is also involved in hepatocyte protection

Finally, we wanted to know whether the ERK-CREB signaling pathway was also implicated in hepatocyte apoptosis and mitochondrial homeostasis. First, TUNEL assays demonstrated that the number of TUNEL-positive hepatocytes was increased in PA-treated cells and was reduced in response to Sirt3 overexpression (Fig. 8A–B). However, blockade of the ERK-CREB signalling pathway re-elevated the ratio of TUNEL-positive cells despite overexpression of Sirt3 (Fig. 8A–B). Similarly, the inflammatory factors, such as TNF α , IL-6 and MCP1, were

also upregulated in PA-treated cells and were decreased to near-normal levels in response to Sirt3 overexpression in an ERK-CREB signalling pathway activation-dependent manner (Fig. 8C–F).

Regarding mitochondrial homeostasis, PA-repressed ATP production was also reversed by Sirt3 overexpression via activating the ERK-CREB axis (Fig. 8G). In addition, PA-triggered ROS production was also reduced by Sirt3, and this effect was nullified by inhibiting the ERK-CREB signalling pathway (Fig. 8H–I). Taken together, these data indicated that the ERK-CREB signalling pathway was also involved in mitochondrial homeostasis and hepatocyte protection in the setting of high-fat stress.

4. Discussion

In the present study, our results suggested that Sirt3 was down-regulated by chronic hyperlipidaemia stress. However, gain-of-function assays of Sirt3 in vitro and in vivo confirmed that Sirt3 played a protective role against fatty liver disease. Mechanistically, Sirt3 overexpression maintained mitochondrial function, reduced mitochondria oxidative stress, sustained mitochondrial energy metabolism, stabilised mitochondrial potential, repressed mitochondrial pro-apoptotic factor liberation, and blocked mitochondrial apoptosis activation. Furthermore, a functional investigation showed that Sirt3 protected mitochondria against high-fat stress via activating mitophagy. Higher Sirt3 was associated with increased Bnip3 expression, which elevated mitophagy. Well-orchestrated mitophagy removed the damaged mitochondria in a timely manner, reducing mitochondrial damage and hepatocyte apoptosis. Finally, our data demonstrated that Sirt3

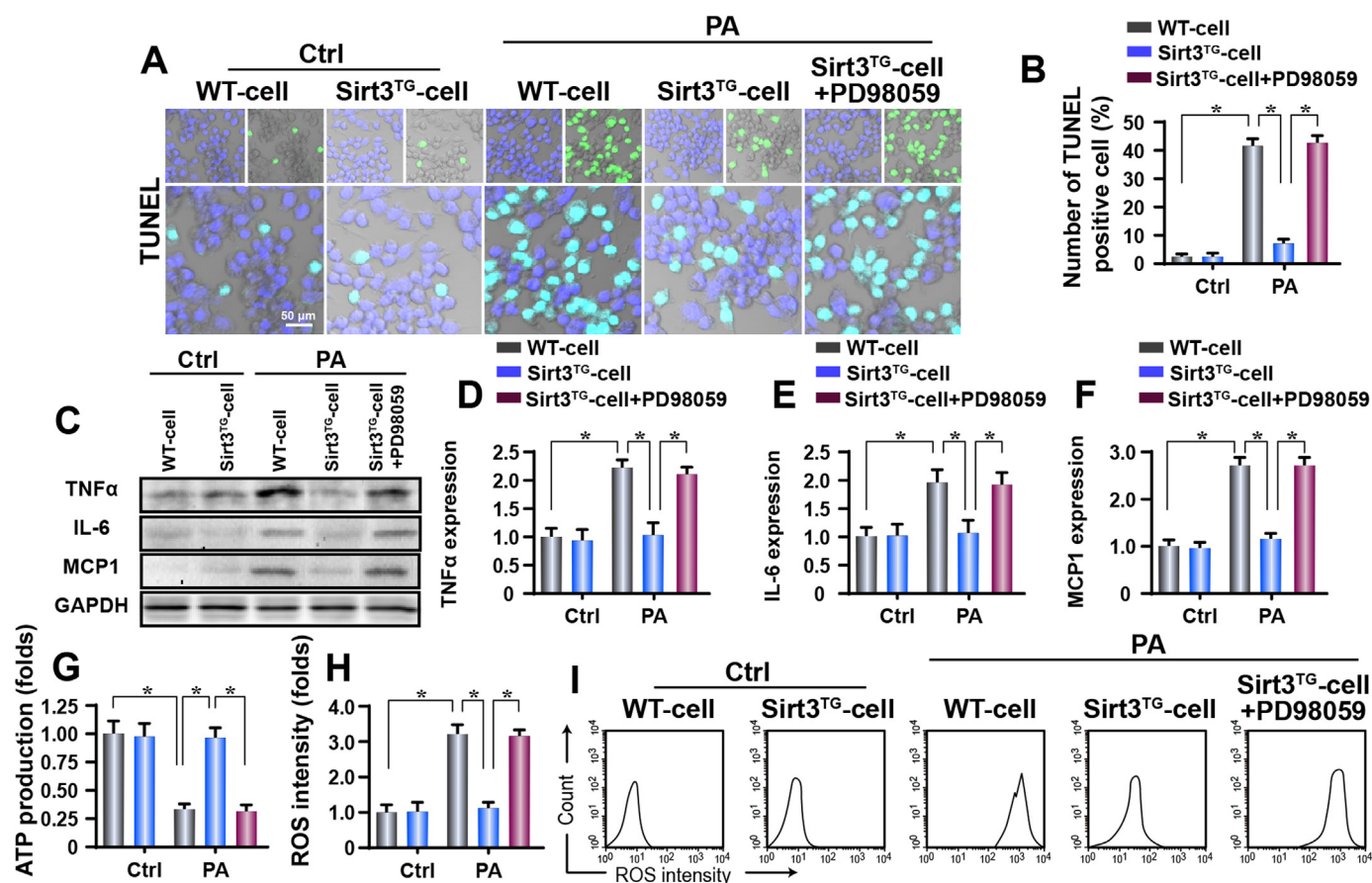


Fig. 8. The ERK-CREB signalling pathway is involved in PA-mediated hepatocyte apoptosis. A–B. TUNEL assay was used to observe the apoptotic index of hepatocytes with ERK inhibition using PD98059. The number of apoptotic cells was recorded. C–F. Western blotting for the inflammatory response via measuring the levels of inflammatory factors. G. ATP production in Sirt3-overexpressed cells with ERK inhibition. H–I. ROS production was measured via flow cytometry. The data represent the mean \pm SEM (n = 4 mice per group). *P < 0.05.

regulated Bnip3-related mitophagy via the ERK-CREB signalling pathway; blockade of the ERK-CREB axis repressed mitophagy activity and abrogated Sirt3-mediated mitochondrial protection as well as hepatocyte survival. As far as we know, this is the first investigation to establish the protective role of Sirt3 in diet-induced fatty liver disease via modifying mitochondrial homeostasis, Bnip3-related mitophagy and the ERK-CREB signalling pathway.

Both loss- and gain-of-function experiments have established the protective role of Sirt3 in mitochondria. For example, Sirt3 prevents hepatocyte mitochondria against oxidative injury via modulating the Ku70/Drp1 signalling pathway [53]. In addition, Sirt3 also maintains osteoblast differentiation via regulating mitochondrial stress [54]. In cardiac disorder, Sirt3 deficiency promotes myocardial remodelling due to mitochondrial dysfunction and defective mitophagy [55]. Furthermore, activation of Sirt3 via Exendin-4 enhances mitochondrial bioenergetics in human adipocytes [52,56]. Similarly, Sirt3 deletion aggravates cardiac ischaemia-reperfusion injury via increasing mPTP opening and mitochondrial DNA damage [57,58]. These results reveal the critical role that Sirt3 played in maintaining mitochondrial homeostasis. In the present study, we found that fatty liver disease was associated with downregulated Sirt3. Loss of Sirt3 was followed by redox imbalance, energy shortage, mitochondrial potential reduction, and the activation of caspase-9-mediated apoptosis in hepatocytes. These data suggest that high-fat-mediated hepatocyte damage results from mitochondrial dysfunction and that Sirt3 downregulation could be considered a pathogenic factor for diet-induced liver illness. Given the protective action of Sirt3 on mitochondria and hyperlipidaemia-challenged hepatocytes [59,60], stimulation of Sirt3 could represent a novel modality to inhibit the progression of fatty liver disease.

Mitophagy, a kind of mitochondrial autophagy, plays an important role in timely removal of damaged mitochondria and recycling of mitochondrial mass [61,62]. The drop in mitophagy activity has been acknowledged as an aetiology for several diseases [63,64]. In acute cardiac reperfusion, defective mitophagy activity results in failure to maintain the mitochondrial mass [65], leading to the accumulation of poorly structured mitochondria and the activation of mitochondrial apoptosis [66,67]. Similarly, in liver cancer and gastric cancer, defective mitophagy is associated with cancer migration inhibition due to energy disorders. In addition, in neurodegenerative diseases, such as Alzheimer's disease and Parkinson's syndrome, aberrant mitophagy promotes neuron injury because of the accumulation of damaged mitochondria [34]. These data have substantiated the sufficiency of pathogenically relevant degrees of impaired mitophagy to induce mitochondria damage, as well as the necessity of mitophagy inhibition for the development of acute and/or chronic metabolic disorders. In the present study, our results illustrated that mitophagy was inhibited by high-fat treatment due to the downregulation of Sirt3. Re-introduction of Sirt3 reversed mitophagy via the activation of Bnip3 expression, enhancing the resistance of mitochondria and hepatocytes to lipotoxicity. These data were similar to those described in a previous study that shows that the activation of Bnip3 elevates mitophagy activity and reduces fatty liver disease. Therefore, interventions to increase either the mitophagy activity or Bnip3 expression during high-fat-diet appear to be protective for liver and mitochondria.

At the molecular levels, we confirmed that Bnip3-mediated mitophagy was regulated by Sirt3 via the ERK-CREB signalling pathway. The ERK-CREB axis is the pro-survival signal for several kinds of diseases, including endothelial oxidative damage, neuronal cell excitotoxicity [68], chronic inflammatory visceral pain, lung cancer death, and retinal pigment epithelial cells oxidative injury [69]. ERK-CREB axis has been found to be the downstream effector of Sirt3, suggesting that Sirt3 could indirectly regulate ERK-CREB pathway [70]. Interestingly, other studies have also reported that ERK-CREB cascade could be handled by Sirt1 [71], suggesting that Sirt3 may indirectly modulate ERK-CREB pathway with the help of other sirtuins. In addition, the regulatory effects of the ERK-CREB axis on mitophagy

management has been established by several studies [72,73]. For example, in the mouse model of myocardial infarction, mitophagy inhibition is attributable to CREB inactivation [33]. In neuroinflammation, activation of the ERK-CREB cascade elevates mitophagy activity and confers additional pro-survival advantages to neurons in response to TNF α stress [25,74]. In accordance with the above findings, our results also confirm that the ERK-CREB axis is beneficial for fatty liver disease: activated ERK-CREB signalling rescues mitophagy activity, sustaining mitochondrial homeostasis and reducing hepatocyte apoptosis. Notably, mitophagy activity is also regulated by other molecules, such as FUNDC1 [26], Parkin [75], and Mfn2 [12]. The role of other mitophagy regulators in fatty liver disease requires further investigation.

In summary, Sirt3 has a liver protective effect against fatty liver disease. Sirt3 activates the ERK-CREB signalling pathway, and the latter upregulates Bnip3-mediated mitophagy, thereby attenuating mitochondrial damage and inhibiting mitochondria-dependent hepatocyte apoptosis. This finding may highlight a new entry point for treating diet-induced fatty liver disease by targeting the Sirt3-ERK-CREB-Bnip3-mitophagy signalling axis. The limitation of this study is that all experiments were done in global Sirt3 transgenic mice. The effects of liver specific Sirt3 overexpression (such as transfection of Sirt3-adenoviral vectors into liver tissues) will provide more solid evidence to support our conclusions.

Acknowledgements

Not applicable.

Availability of data and materials

All data generated or analysed during this study are included in this published article.

Authors contribution

RBL and HZ conceived the research; RBL, TX, DDL, HZ and CBW performed the experiments; all authors participated in discussing and revising the manuscript.

Ethical approval and consent to participate

The animal study was performed in accordance with the Declaration of Helsinki. All experimental protocols were approved by the Ethics Committee of Chinese PLA General Hospital and the Animal Care and Use Committee of Chinese PLA General Hospital, Beijing, China. The ethics reference number: PLA-2016-S332GHC.

Competing interests

The authors declare they have no conflict of interest.

References

- [1] Z. Hu, J. Cheng, J. Xu, W. Ruf, C.J. Lockwood, Tissue factor is an angiogenic-specific receptor for factor VII-targeted immunotherapy and photodynamic therapy, *Angiogenesis* 20 (1) (2017) 85–96.
- [2] S.H. Chang, Y.H. Yeh, J.L. Lee, Y.J. Hsu, C.T. Kuo, W.J. Chen, Transforming growth factor-beta-mediated CD44/STAT3 signaling contributes to the development of atrial fibrosis and fibrillation, *Basic Res. Cardiol.* 112 (5) (2017) 58.
- [3] F. Dufour, T. Rattier, S. Shirley, G. Picarda, A.A. Constantinescu, A. Morle, A.B. Zakaria, G. Marcion, S. Causse, E. Szegezdi, D.M. Zajonc, R. Seigneuric, G. Guichard, T. Gharbi, F. Picaud, G. Herlem, C. Garrido, P. Schneider, C.A. Benedict, O. Micheau, N-glycosylation of mouse TRAIL-R and human TRAIL-R1 enhances TRAIL-induced death, *Cell Death Differ.* 24 (3) (2017) 500–510.
- [4] D. Feng, B. Wang, L. Wang, N. Abraham, K. Tao, L. Huang, W. Shi, Y. Dong, Y. Qu, Pre-ischemia melatonin treatment alleviated acute neuronal injury after ischemic stroke by inhibiting endoplasmic reticulum stress-dependent autophagy via PERK and IRE1 signalings, *J. Pineal Res.* 62 (3) (2017).

- [5] C.H.T. Boone, R.A. Grove, D. Adamcova, J. Seravalli, J. Adamec, Oxidative stress, metabolomics profiling, and mechanism of local anesthetic induced cell death in yeast, *Redox Biol.* 12 (2017) 139–149.
- [6] T.D. Le Cras, P.S. Moberley-Schuman, M. Broering, L. Fei, C.C. Trenor 3rd, D.M. Adams, Angiopoietins as serum biomarkers for lymphatic anomalies, *Angiogenesis* 20 (1) (2017) 163–173.
- [7] W.R. Garcia-Nino, F. Correa, J.I. Rodriguez-Barrera, J.C. Leon-Contreras, M. Buelna-Chontal, E. Soria-Castro, R. Hernandez-Pando, J. Pedraza-Chaverri, C. Zazueta, Cardioprotective kinase signaling to subsarcolemmal and interfibrillar mitochondria is mediated by caveolar structures, *Basic Res. Cardiol.* 112 (2) (2017) 15.
- [8] P.S. Murphy, J. Wang, S.P. Bhagwat, J.C. Munger, W.J. Janssen, T.W. Wright, M.R. Elliott, CD73 regulates anti-inflammatory signaling between apoptotic cells and endotoxin-conditioned tissue macrophages, *Cell Death Differ.* 24 (3) (2017) 559–570.
- [9] Y. Gao, X. Xiao, C. Zhang, W. Yu, W. Guo, Z. Zhang, Z. Li, X. Feng, J. Hao, K. Zhang, B. Xiao, M. Chen, W. Huang, S. Xiong, X. Wu, W. Deng, Melatonin synergizes the chemotherapeutic effect of 5-fluorouracil in colon cancer by suppressing PI3K/AKT and NF-kappaB/iNOS signaling pathways, *J. Pineal Res.* 62 (2) (2017).
- [10] A. Daiber, M. Oelze, S. Steven, S. Kroller-Schon, T. Munzel, Taking up the cudgels for the traditional reactive oxygen and nitrogen species detection assays and their use in the cardiovascular system, *Redox Biol.* 12 (2017) 35–49.
- [11] Q. Chen, T. Wang, J. Li, S. Wang, F. Qiu, H. Yu, Y. Zhang, Effects of natural products on fructose-induced nonalcoholic fatty liver disease (NAFLD), *Nutrients* 9 (2) (2017).
- [12] H. Zhou, S. Wang, S. Hu, Y. Chen, J. Ren, ER-mitochondria microdomains in cardiac ischemia-reperfusion injury: a fresh perspective, *Front. Physiol.* 9 (2018) 755.
- [13] H. Zhu, Q. Jin, Y. Li, Q. Ma, J. Wang, D. Li, H. Zhou, Y. Chen, Melatonin protected cardiac microvascular endothelial cells against oxidative stress injury via suppression of IP3R-[Ca²⁺]_i/VDAC-[Ca²⁺]_m axis by activation of MAPK/ERK signaling pathway, *Cell Stress Chaperones* 23 (1) (2018) 101–113.
- [14] Y. Zhang, H. Zhou, W. Wu, C. Shi, S. Hu, T. Yin, Q. Ma, T. Han, Y. Zhang, F. Tian, Y. Chen, Liraglutide protects cardiac microvascular endothelial cells against hypoxia/reoxygenation injury through the suppression of the SR-Ca(2+)-XO-ROS axis via activation of the GLP-1R/PI3K/Akt/survivin pathways, *Free Radic. Biol. Med.* 95 (2016) 278–292.
- [15] J. Ligeza, P. Marona, N. Gach, B. Lipert, K. Miekus, W. Wilk, J. Jaszczynski, A. Stelmach, A. Loboda, J. Dulak, W. Braniccki, J. Rys, J. Jura, MCP1P1 contributes to clear cell renal cell carcinomas development, *Angiogenesis* 20 (3) (2017) 325–340.
- [16] W. Sun, L. Zhao, X. Song, J. Zhang, Y. Xing, N. Liu, Y. Yan, Z. Li, Y. Lu, J. Wu, L. Li, Y. Xiao, X. Tian, T. Li, Y. Guan, Y. Wang, B. Liu, MicroRNA-210 modulates the cellular energy metabolism shift during H₂O₂-induced oxidative stress by repressing ISCU in H9c2 cardiomyocytes, *Cell. Physiol. Biochem.* 43 (1) (2017) 383–394.
- [17] M.L. Chen, X.H. Zhu, L. Ran, H.D. Lang, L. Yi, M.T. Mi, Trimethylamine-N-oxide induces vascular inflammation by activating the NLRP3 inflammasome through the SIRT3-SOD2-mtROS signaling pathway, *J. Am. Heart Assoc.* 6 (9) (2017).
- [18] M. Zhai, B. Li, W. Duan, L. Jing, B. Zhang, M. Zhang, L. Yu, Z. Liu, B. Yu, K. Ren, E. Gao, Y. Yang, H. Liang, Z. Jin, S. Yu, Melatonin ameliorates myocardial ischemia reperfusion injury through SIRT3-dependent regulation of oxidative stress and apoptosis, *J. Pineal Res.* 63 (2) (2017).
- [19] G.E. Wang, Y.F. Li, Y.J. Zhai, L. Gong, J.Y. Tian, M. Hong, N. Yao, Y.P. Wu, H. Kurihara, R.R. He, Theacrine protects against nonalcoholic fatty liver disease by regulating acylcarnitine metabolism, *Metabolism* (2018).
- [20] P. Thirusangu, V. Vigneshwaran, T. Prashanth, B.R. Vijay Avin, V.H. Malojirao, H. Rakesh, S.A. Khanum, R. Mahmood, B.T. Prabhakar, BP-1T, an antiangiogenic benzophenone-thiazole pharmacophore, counteracts HIF-1 signalling through p53/MDM2-mediated HIF-1alpha proteasomal degradation, *Angiogenesis* 20 (1) (2017) 55–71.
- [21] J. Xu, Y. Wu, G. Lu, S. Xie, Z. Ma, Z. Chen, H.M. Shen, D. Xia, Importance of ROS-mediated autophagy in determining apoptotic cell death induced by physalbin B, *Redox Biol.* 12 (2017) 198–207.
- [22] C. Sarkar, R.K. Ganju, V.J. Pompili, D. Chakroborty, Enhanced peripheral dopamine impairs post-ischemic healing by suppressing angiotensin receptor type 1 expression in endothelial cells and inhibiting angiogenesis, *Angiogenesis* 20 (1) (2017) 97–107.
- [23] L. Xiao, X. Xu, F. Zhang, M. Wang, Y. Xu, D. Tang, J. Wang, Y. Qin, Y. Liu, C. Tang, L. He, A. Greka, Z. Zhou, F. Liu, Z. Dong, L. Sun, The mitochondria-targeted antioxidant MitoQ ameliorated tubular injury mediated by mitophagy in diabetic kidney disease via Nrf2/PINK1, *Redox Biol.* 11 (2017) 297–311.
- [24] H. Zhou, P. Zhu, J. Wang, H. Zhu, J. Ren, Y. Chen, Pathogenesis of cardiac ischemia reperfusion injury is associated with CK2alpha-disturbed mitochondrial homeostasis via suppression of FUNDC1-related mitophagy, *Cell Death Differ.* 25 (6) (2018) 1080–1093.
- [25] H. Li, F. He, X. Zhao, Y. Zhang, X. Chu, C. Hua, Y. Qu, Y. Duan, L. Ming, YAP inhibits the apoptosis and migration of human rectal cancer cells via suppression of JNK-Drp1-mitochondrial fission-HtrA2/Omi pathways, *Cell. Physiol. Biochem.* 44 (5) (2017) 2073–2089.
- [26] H. Zhou, J. Wang, P. Zhu, H. Zhu, S. Toan, S. Hu, J. Ren, Y. Chen, NR4A1 aggravates the cardiac microvascular ischemia reperfusion injury through suppressing FUNDC1-mediated mitophagy and promoting Mff-required mitochondrial fission by CK2alpha, *Basic Res. Cardiol.* 113 (4) (2018) 23.
- [27] J.C. Mayo, R.M. Sainz, P. Gonzalez Menendez, V. Cepas, D.X. Tan, R.J. Reiter, Melatonin and sirtuins: a "not-so unexpected" relationship, *J. Pineal Res.* 62 (2) (2017).
- [28] F. Sigala, P. Efentakis, D. Karageorgiadi, K. Filis, P. Zampas, E.K. Iliodromitis, G. Zografos, A. Papapetropoulos, I. Andreadou, Reciprocal regulation of eNOS, H2S and CO-synthesizing enzymes in human atheroma: correlation with plaque stability and effects of simvastatin, *Redox Biol.* 12 (2017) 70–81.
- [29] H. Zhou, W. Du, Y. Li, C. Shi, N. Hu, S. Ma, W. Wang, J. Ren, Effects of melatonin on fatty liver disease: the role of NR4A1/DNA-PKcs/p53 pathway, mitochondrial fission, and mitophagy, *J. Pineal Res.* 64 (1) (2018).
- [30] E. Nunez-Gomez, M. Pericacho, C. Ollauri-Ibanez, C. Bernabeu, J.M. Lopez-Novoa, The role of endoglin in post-ischemic revascularization, *Angiogenesis* 20 (1) (2017) 1–24.
- [31] H.J. Lee, Y.H. Jung, G.E. Choi, S.H. Ko, S.J. Lee, S.H. Lee, H.J. Han, BNIP3 induction by hypoxia stimulates FASN-dependent free fatty acid production enhancing therapeutic potential of umbilical cord blood-derived human mesenchymal stem cells, *Redox Biol.* 13 (2017) 426–443.
- [32] D. Glick, W. Zhang, M. Beaton, G. Marsboom, M. Gruber, M.C. Simon, J. Hart, G.W. Dorn 2nd, M.J. Brady, K.F. Macleod, BNIP3 regulates mitochondrial function and lipid metabolism in the liver, *Mol. Cell. Biol.* 32 (13) (2012) 2570–2584.
- [33] S. Wu, Q. Lu, Q. Wang, Y. Ding, Z. Ma, X. Mao, K. Huang, Z. Xie, M.H. Zou, Binding of FUN14 domain containing 1 with inositol 1,4,5-trisphosphate receptor in mitochondria-associated endoplasmic reticulum membranes maintains mitochondrial dynamics and function in hearts in vivo, *Circulation* 136 (23) (2017) 2248–2266.
- [34] Q. Lei, J. Tan, S. Yi, N. Wu, Y. Wang, H. Wu, Mitochondrial acid 5 activates the MAPK-ERK-yap signaling pathways to protect mouse microglial BV-2 cells against TNFalpha-induced apoptosis via increased Bnip3-related mitophagy, *Cell. Mol. Biol. Lett.* 23 (2018) 14.
- [35] M. Ackermann, Y.O. Kim, W.L. Wagner, D. Schuppan, C.D. Valenzuela, S.J. Mentzer, S. Kreuz, D. Stiller, L. Wollin, M.A. Konerding, Effects of nintedanib on the microvascular architecture in a lung fibrosis model, *Angiogenesis* 20 (3) (2017) 359–372.
- [36] H. Zhou, Y. Yue, J. Wang, Q. Ma, Y. Chen, Melatonin therapy for diabetic cardiomyopathy: a mechanism involving Syk-mitochondrial complex I-SERCA pathway, *Cell Signal.* 47 (2018) 88–100.
- [37] N.J.R. Blackburn, B. Vulesevic, B. Mcneill, C.E. Cimenci, A. Ahmadi, M. Gonzalez-Gomez, A. Ostojic, Z. Zhong, M. Brownlee, P.J. Beisswenger, R.W. Milne, E.J. Suuronen, Methylglyoxal-derived advanced glycation end products contribute to negative cardiac remodeling and dysfunction post-myocardial infarction, *Basic Res. Cardiol.* 112 (5) (2017) 57.
- [38] H. Zhou, C. Shi, S. Hu, H. Zhu, J. Ren, Y. Chen, BII is associated with microvascular protection in cardiac ischemia reperfusion injury via repressing Syk-Nox2-Drp1-mitochondrial fission pathways, *Angiogenesis* 21 (3) (2018) 599–615.
- [39] D. Brasacchio, A.E. Alsop, T. Noori, M. Lufti, S. Iyer, K.J. Simpson, P.I. Bird, R.M. Kluck, R.W. Johnstone, J.A. Trapani, Epigenetic control of mitochondrial cell death through PACS1-mediated regulation of BAX/BAK oligomerization, *Cell Death Differ.* 24 (6) (2017) 961–970.
- [40] H. Zhou, J. Wang, P. Zhu, S. Hu, J. Ren, Ripk3 regulates cardiac microvascular reperfusion injury: the role of IP3R-dependent calcium overload, XO-mediated oxidative stress and F-actin/filopodia-based cellular migration, *Cell Signal.* 45 (2018) 12–22.
- [41] Q. Jin, R. Li, N. Hu, T. Xin, P. Zhu, S. Hu, S. Ma, H. Zhu, J. Ren, H. Zhou, DUSP1 alleviates cardiac ischemia/reperfusion injury by suppressing the Mff-required mitochondrial fission and Bnip3-related mitophagy via the JNK pathways, *Redox Biol.* 14 (2018) 576–587.
- [42] A.F. Alghanem, E.L. Wilkinson, M.S. Emmett, M.A. Aljasir, K. Holmes, B.A. Rothermel, V.A. Simms, V.L. Heath, M.J. Cross, RCAN1.4 regulates VEGFR-2 internalisation, cell polarity and migration in human microvascular endothelial cells, *Angiogenesis* 20 (3) (2017) 341–358.
- [43] A.K. Gadicherla, N. Wang, M. Bulic, E. Agullo-Pascual, A. Lissoni, M. De Smet, M. Delmar, G. Bultynck, D.V. Krysko, A. Camara, K.D. Schluter, R. Schulz, W.M. Kwok, L. Leybaert, Mitochondrial Cx43 hemichannels contribute to mitochondrial calcium entry and cell death in the heart, *Basic Res. Cardiol.* 112 (3) (2017) 27.
- [44] H. Zhou, S. Wang, P. Zhu, S. Hu, Y. Chen, J. Ren, Empagliflozin rescues diabetic myocardial microvascular injury via AMPK-mediated inhibition of mitochondrial fission, *Redox Biol.* 15 (2018) 335–346.
- [45] J.A. Glab, M. Doerflinger, C. Nedeva, I. Jose, G.W. Mbogo, J.C. Paton, A.W. Paton, A.J. Kueh, M.J. Herold, D.C. Huang, D. Segal, G. Brumatti, H. Puthalakath, DR5 and caspase-8 are dispensable in ER stress-induced apoptosis, *Cell Death Differ.* 24 (5) (2017) 944–950.
- [46] J.A. Couto, U.M. Ayturk, D.J. Konczyk, J.A. Goss, A.Y. Huang, S. Hann, J.L. Reeve, M.G. Liang, J. Bischoff, M.L. Warman, A.K. Greene, A somatic GNAI1 mutation is associated with extremity capillary malformation and overgrowth, *Angiogenesis* 20 (3) (2017) 303–306.
- [47] M. Rienks, P. Carai, N. Bitsch, M. Schellings, M. Vanhaverbeke, J. Verjans, I. Cuijpers, S. Heymans, A. Papageorgiou, Sema3A promotes the resolution of cardiac inflammation after myocardial infarction, *Basic Res. Cardiol.* 112 (4) (2017) 42.
- [48] P. Zhu, S. Hu, Q. Jin, D. Li, F. Tian, S. Toan, Y. Li, H. Zhou, Y. Chen, Ripk3 promotes ER stress-induced necroptosis in cardiac IR injury: a mechanism involving calcium overload/XO/ROS/mPTP pathway, *Redox Biol.* 16 (2018) 157–168.
- [49] H. Zhou, D. Li, P. Zhu, Q. Ma, S. Toan, J. Wang, S. Hu, Y. Chen, Y. Zhang, Inhibitory effect of melatonin on necroptosis via repressing the Ripk3-PGAM5-CypD-mPTP pathway attenuates cardiac microvascular ischemia-reperfusion injury, *J. Pineal Res.* (2018) e12503.
- [50] H. Zhou, Q. Ma, P. Zhu, J. Ren, R.J. Reiter, Y. Chen, Protective role of melatonin in cardiac ischemia-reperfusion injury: from pathogenesis to targeted therapy, *J. Pineal Res.* 64 (3) (2018).
- [51] C. Shi, Y. Cai, Y. Li, Y. Li, N. Hu, S. Ma, S. Hu, P. Zhu, W. Wang, H. Zhou, Yap

- promotes hepatocellular carcinoma metastasis and mobilization via governing cofilin/F-actin/lamellipodium axis by regulation of JNK/Bnip3/SERCA/CaMKII pathways, *Redox Biol.* 14 (2018) 59–71.
- [52] H.R. Griffiths, D. Gao, C. Pararasa, Redox regulation in metabolic programming and inflammation, *Redox Biol.* 12 (2017) 50–57.
- [53] J.M. Garcia-Ruiz, C. Galan-Arriola, R. Fernandez-Jimenez, J. Aguero, J. Sanchez-Gonzalez, A. Garcia-Alvarez, M. Nuno-Ayala, G.P. Dube, Z. Zafirelis, G.J. Lopez-Martin, J.A. Bernal, E. Lara-Pezzi, V. Fuster, B. Ibanez, Bloodless reperfusion with the oxygen carrier HBOC-201 in acute myocardial infarction: a novel platform for cardioprotective probes delivery, *Basic Res. Cardiol.* 112 (2) (2017) 17.
- [54] J. Gao, Z. Feng, X. Wang, M. Zeng, J. Liu, S. Han, J. Xu, L. Chen, K. Cao, J. Long, Z. Li, W. Shen, J. Liu, SIRT3/SOD2 maintains osteoblast differentiation and bone formation by regulating mitochondrial stress, *Cell Death Differ.* 25 (2) (2018) 229–240.
- [55] T. Wei, G. Huang, J. Gao, C. Huang, M. Sun, J. Wu, J. Bu, W. Shen, Sirtuin 3 deficiency accelerates hypertensive cardiac remodeling by impairing angiogenesis, *J. Am. Heart Assoc.* 6 (8) (2017).
- [56] S.N. Schock, N.V. Chandra, Y. Sun, T. Irie, Y. Kitagawa, B. Gotoh, L. Coscoy, A. Winoto, Induction of necroptotic cell death by viral activation of the RIG-I or STING pathway, *Cell Death Differ.* 24 (4) (2017) 615–625.
- [57] D. Iggena, Y. Winter, B. Steiner, Melatonin restores hippocampal neural precursor cell proliferation and prevents cognitive deficits induced by jet lag simulation in adult mice, *J. Pineal Res.* 62 (4) (2017).
- [58] H. Hong, T. Tao, S. Chen, C. Liang, Y. Qiu, Y. Zhou, R. Zhang, MicroRNA-143 promotes cardiac ischemia-mediated mitochondrial impairment by the inhibition of protein kinase Cepsilon, *Basic Res. Cardiol.* 112 (6) (2017) 60.
- [59] V. Jahandiez, M. Cour, T. Bochaton, M. Abrial, J. Loufouat, A. Gharib, A. Varennes, M. Ovize, L. Argaud, Fast therapeutic hypothermia prevents post-cardiac arrest syndrome through cyclophilin D-mediated mitochondrial permeability transition inhibition, *Basic Res. Cardiol.* 112 (4) (2017) 35.
- [60] W.S. Hambright, R.S. Fonseca, L. Chen, R. Na, Q. Ran, Ablation of ferroptosis regulator glutathione peroxidase 4 in forebrain neurons promotes cognitive impairment and neurodegeneration, *Redox Biol.* 12 (2017) 8–17.
- [61] H.Y. Lee, K. Back, Melatonin is required for H₂O₂- and NO-mediated defense signaling through MAPKKK3 and OX1 in *Arabidopsis thaliana*, *J. Pineal Res.* 62 (2) (2017).
- [62] J.R. Kingery, T. Hamid, R.K. Lewis, M.A. Ismahil, S.S. Bansal, G. Rokosh, T.M. Townes, S.T. Ildstad, S.P. Jones, S.D. Prabhu, Leukocyte iNOS is required for inflammation and pathological remodeling in ischemic heart failure, *Basic Res. Cardiol.* 112 (2) (2017) 19.
- [63] M. Merjaneh, A. Langlois, S. Larochele, C.B. Cloutier, S. Ricard-Blum, V.J. Moulin, Pro-angiogenic capacities of microvesicles produced by skin wound myofibroblasts, *Angiogenesis* 20 (3) (2017) 385–398.
- [64] K. Lee, K. Back, Overexpression of rice serotonin N-acetyltransferase 1 in transgenic rice plants confers resistance to cadmium and senescence and increases grain yield, *J. Pineal Res.* 62 (3) (2017).
- [65] H. Zhou, D. Li, P. Zhu, S. Hu, N. Hu, S. Ma, Y. Zhang, T. Han, J. Ren, F. Cao, Y. Chen, Melatonin suppresses platelet activation and function against cardiac ischemia/reperfusion injury via PPARgamma/FUNDC1/mitophagy pathways, *J. Pineal Res.* 63 (4) (2017).
- [66] B. Kalyanaraman, Teaching the basics of cancer metabolism: developing antitumor strategies by exploiting the differences between normal and cancer cell metabolism, *Redox Biol.* 12 (2017) 833–842.
- [67] P.T. Kang, C.L. Chen, P. Lin, W.M. Chilian, Y.R. Chen, Impairment of pH gradient and membrane potential mediates redox dysfunction in the mitochondria of the post-ischemic heart, *Basic Res. Cardiol.* 112 (4) (2017) 36.
- [68] K. Lee, C. Park, Y. Oh, H. Lee, J. Cho, Antioxidant and neuroprotective effects of N-((3,4-dihydro-2H-benzo[h]chromen-2-yl)methyl)-4-methoxyaniline in primary cultured rat cortical cells: involvement of ERK-CREB signaling, *Molecules* 23 (3) (2018).
- [69] C.M. Chong, W. Zheng, Artemisinin protects human retinal pigment epithelial cells from hydrogen peroxide-induced oxidative damage through activation of ERK/CREB signaling, *Redox Biol.* 9 (2016) 50–56.
- [70] N.R. Sundaresan, M. Gupta, G. Kim, S.B. Rajamohan, A. Isbatan, M.P. Gupta, Sirt3 blocks the cardiac hypertrophic response by augmenting Foxo3a-dependent antioxidant defense mechanisms in mice, *J. Clin. Investig.* 119 (9) (2009) 2758–2771.
- [71] Z. Safaiejad, M. Nabiuni, M. Peymani, K. Ghaedi, M.H. Nasr-Esfahani, H. Baharvand, Resveratrol promotes human embryonic stem cells self-renewal by targeting SIRT1-ERK signaling pathway, *Eur. J. Cell Biol.* 96 (7) (2017) 665–672.
- [72] Z. Liu, L. Gan, Y. Xu, D. Luo, Q. Ren, S. Wu, C. Sun, Melatonin alleviates inflammasome-induced pyroptosis through inhibiting NF-kappaB/GSDMD signal in mice adipose tissue, *J. Pineal Res.* 63 (1) (2017).
- [73] D. Liu, X. Zeng, X. Li, J.L. Mehta, X. Wang, Role of NLRP3 inflammasome in the pathogenesis of cardiovascular diseases, *Basic Res. Cardiol.* 113 (1) (2017) 5.
- [74] A.V. Kozlov, J.R. Lancaster Jr., A.T. Meszaros, A. Weidinger, Mitochondria-mediated pathways of organ failure upon inflammation, *Redox Biol.* 13 (2017) 170–181.
- [75] H. Zhou, Y. Zhang, S. Hu, C. Shi, P. Zhu, Q. Ma, Q. Jin, F. Cao, F. Tian, Y. Chen, Melatonin protects cardiac microvasculature against ischemia/reperfusion injury via suppression of mitochondrial fission-VDAC1-HK2-mPTP-mitophagy axis, *J. Pineal Res.* 63 (1) (2017).